



Entropy production of nonreciprocal interactions

Ziluo Zhang (张子洛)^{1,2} and Rosalba Garcia-Millan^{3,4,*}

¹*Department of Mathematics, Imperial College London, London SW7 2AZ, United Kingdom*

²*Wenzhou Institute, University of Chinese Academy of Sciences, Wenzhou, Zhejiang 325001, China*

³*DAMTP, Centre for Mathematical Sciences, University of Cambridge, Cambridge CB3 0WA, United Kingdom*

⁴*St John's College, University of Cambridge, Cambridge CB2 1TP, United Kingdom*



(Received 25 November 2022; accepted 13 April 2023; published 17 May 2023)

Nonreciprocal interactions are present in many systems out of equilibrium. The rate of entropy production is a measure that quantifies the time irreversibility of a system, and thus how far it is from equilibrium. In this work, we introduce a nonmotile active particle system where activity originates from asymmetric, pairwise interaction forces that result in an injection of energy at the microscopic scale. We calculate stationary correlation functions and entropy production rate in three exactly solvable cases, and analyze a more general case in a perturbation theory as an expansion in weak interactions. Our results show that equilibrium may be recovered by adjusting the diffusion constants despite nonreciprocity, revealing an equivalence in the absolute amplitude of the force and diffusivity. We support our analytical results with numerical simulations.

DOI: [10.1103/PhysRevResearch.5.L022033](https://doi.org/10.1103/PhysRevResearch.5.L022033)

Introduction. Nonreciprocal interactions are those that do not obey Newton's third law (*actio equal reactio*). These generate intrinsically out-of-equilibrium dynamics [1–4] and are often invoked to model striking dynamical pattern formation such as flocking [5,6], worming [7], or traveling states [8]. Common mechanisms that break reciprocity are (anti-)alignment [9] and vision cone interactions [10–12]. Nonreciprocal interactions between two species play a crucial role in numerous biological processes, such as predator-prey dynamics [13,14] or collective cell migration [15]. Nonreciprocity is found in attractive-repulsive interactions giving rise, for example, to the chase-and-run dynamics present between a dog and a herd of sheep: while the dog runs toward the sheep, sheep fearfully run away from the dog, following a trajectory such as the one shown in Fig. 1(a). A remarkable application of nonreciprocal interactions is the experimental design of self-propelling colloids [4,16–19]. The underlying principle of formation and self-propulsion of colloids such as Janus dimers is based on attractive-repulsive interactions between two types of nonmotile microspheres that are sustained by light [16,17], or by ion exchange [18]. The emergence of self-propulsion due to interactions between particles that are otherwise nonmotile indicates that the system is out of equilibrium and that it therefore produces entropy through the dissipation of heat.

Over the last decade, the rate of entropy production \dot{S} has become a prominent measure of irreversibility that quantifies

how far from equilibrium a system is [20–23]. Beyond its binary ability to determine whether a system is in thermal equilibrium ($\dot{S} = 0$) or not ($\dot{S} > 0$), following Sekimoto's thermodynamic interpretation of Langevin dynamics, the entropy production quantifies the average rate of heat dissipation in the medium, or equivalently, the energetic cost of sustaining a nonequilibrium steady state [1,24,25]. Measuring and calculating the entropy production rate is, therefore, key to understanding the nonequilibrium behavior of a system and poses a major theoretical challenge in the case of interacting many-particle active systems. Recent studies have focused on the thermodynamic properties of nonreciprocity in a system described by coupled, linear Langevin equations, where interactions are modeled by harmonic oscillators [1,2,19,26]. References [1,19] showed that there exist systems with nonreciprocal interactions that do satisfy detailed balance under specific conditions. However, a fully microscopic calculation of the entropy production of a many-particle system with nonlinear and nonreciprocal interaction forces is lacking. The power of microscopic theories in the study of active particle systems lies in the direct link they establish between agents' dynamics and their emergent phenomena. Deriving exact results that serve as a benchmark is thus of paramount importance [20,22].

In this Letter, we introduce a nonmotile active particle system that is driven out of equilibrium by nonreciprocal interactions between one particle and the rest [27]. We consider three exactly solvable cases and a fourth, more general case using a perturbative field theory: (a) two-particle system, (b) equilibrium system, (c) chase-and-run dynamics, and (d) sinusoidal interaction potentials. Case (a) is a model for a single Janus dimer under a suitable choice of interaction forces [16–18], whereas cases (b)–(d) involve a single particle of one type, such as a tracer, in a dilute bath of particles of another type under different assumptions on the interaction

*rg646@cam.ac.uk

Published by the American Physical Society under the terms of the [Creative Commons Attribution 4.0 International license](https://creativecommons.org/licenses/by/4.0/). Further distribution of this work must maintain attribution to the author(s) and the published article's title, journal citation, and DOI.

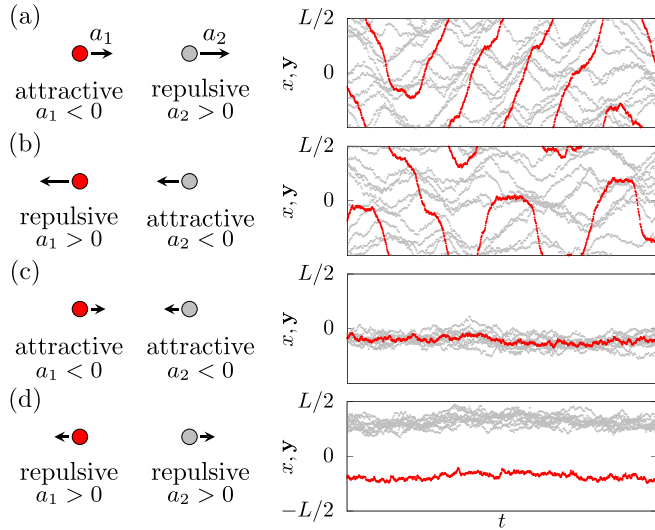


FIG. 1. Particle trajectories (x, y) described by Eq. (1) with one particle of species A (red) and $N = 10$ particles of species B (gray), sinusoidal interacting potentials, equal diffusivities, and zero drifts. The sign of potential amplitudes a_1 and a_2 are indicated on the left. Interactions are nonreciprocal in (a) and (b) and reciprocal in (c) and (d). In this example, since $D_1 = D_2$, nonreciprocal systems are active and reciprocal systems are passive.

forces. In the dilute regime, interactions between particles of the same kind are assumed to be negligible [28–30]. In case (b) we find the condition for detailed balance that interaction forces must satisfy for this system to be at equilibrium. Case (c) explores chase-and-run dynamics, where interaction forces between particles of different kinds are equal in magnitude and have equal direction. This system is a model of predator-prey dynamics [13,14], and collective cell migration [15]. In case (d), we assume that interaction forces are given by a sinusoidal pair potential with variable amplitude and explore the phase space of attractive and repulsive forces. Our perturbative approach provides a systematic framework to calculate correlation functions and the short-time propagator, both of which are essential to calculate the entropy production rate [20,31–33]. Our analytical results are compared with the average rate of dissipated heat along the stochastic trajectories of the particles in Sekimoto’s framework [1,25,34,35], showing good agreement within the domain where our perturbative treatment holds. We address the regime of small to intermediate particle numbers, and establish the path from Langevin dynamics to emergent effective interactions.

Model. We consider a one-dimensional system with two types of particles: one particle of species A at position x and N particles of species B at $\mathbf{y} = (y_1, \dots, y_N)$, with diffusion constants D_1 and D_2 , and drifts u_1 and u_2 , that live on a ring of length L . The interaction forces are mediated by the periodic and bounded pair potentials V_1 and V_2 , resulting in the additional effective drifts $-\sum_i \partial_x V_1(x - y_i)$ for particle A and $-\partial_{y_i} V_2(y_i - x)$ for each particle B. According to the structure of these pair interactions, B particles do not directly interact with each other, although their trajectories are effectively coupled by means of particle A, as we discuss below.

The system dynamics are described by the coupled, overdamped Langevin equations,

$$\dot{x} = u_1 - \sum_{i=1}^N V_1'(x - y_i) + \xi(t), \quad (1a)$$

$$\dot{y}_i = u_2 - V_2'(y_i - x) + \xi_i(t), \quad (1b)$$

where ξ and ξ_i are Gaussian white noises, with correlators $\langle \xi(t)\xi(t') \rangle = 2D_1\delta(t - t')$ and $\langle \xi_i(t)\xi_j(t') \rangle = 2D_2\delta_{i,j}\delta(t - t')$. We assume Boltzmann constant and mobility to be unity, and therefore deem the diffusion constants to essentially be temperatures. The stationary currents are

$$J_x = \left(u_1 - \sum_{i=1}^N V_1'(x - y_i) - D_1\partial_x \right) P(x, \mathbf{y}), \quad (2a)$$

$$J_{y_i} = [u_2 - V_2'(y_i - x) - D_2\partial_{y_i}] P(x, \mathbf{y}), \quad (2b)$$

where $P(x, \mathbf{y})$ is the joint particle density of state x, \mathbf{y} [36]. If interactions are reciprocal, namely, the interaction potentials satisfy $V_1(\ell) = V_2(-\ell) \equiv V(\ell)$ with $\ell = x - y$, then forces are conservative because Eq. (1) can be derived from the Hamiltonian $\mathcal{H} = -u_1x + \sum_{i=1}^N [-u_2y_i + V(x - y_i)]$. Conversely, nonreciprocal interactions result in nonconservative forces. Figure 1 shows particle trajectories described by Eq. (1) with different combinations of attractive and repulsive potentials, illustrating the breakdown of time-reversal symmetry in the active systems in Figs. 1(a) and 1(b), in contrast to the passive systems in Figs. 1(c) and 1(d). We simulate particle trajectories described by Eq. (1) using standard Brownian dynamics simulations.

We calculate the entropy production to quantify the irreversibility of this system [21–23]. In Gaspard’s framework [21], the entropy production of a Markov process is

$$\begin{aligned} \dot{S}(t) = & \lim_{\tau \rightarrow 0} \frac{1}{(N!)^2} \int_0^L dx dx' d^N y d^N y' \\ & \times \left\{ P(x, \mathbf{y}; t) \dot{W}(x, \mathbf{y} \rightarrow x', \mathbf{y}'; \tau) \right. \\ & \left. \times \ln \left(\frac{P(x, \mathbf{y}; t) W(x, \mathbf{y} \rightarrow x', \mathbf{y}'; \tau)}{P(x', \mathbf{y}'; t) W(x', \mathbf{y}' \rightarrow x, \mathbf{y}; \tau)} \right) \right\}, \quad (3) \end{aligned}$$

where $W(x, \mathbf{y} \rightarrow x', \mathbf{y}'; \tau)$ is the transition probability for the system to go from state x, \mathbf{y} to state x', \mathbf{y}' in an interval of time τ . The Gibbs factor $1/N!$ in each integral over \mathbf{y} in Eq. (3) accounts for the phase space of the positions of B particles being that of indistinguishable particles in the continuum, where the probability that two particles are found at the same position has zero measure.

Using the framework established in [20], the entropy production in Eq. (3) in the stationary state simplifies to

$$\begin{aligned} \dot{S} = & \int_0^L dx dy \left\{ -V_1''(x - y) + \frac{1}{D_1} \left(\frac{u_1}{N} - V_1'(x - y) \right)^2 \right. \\ & \left. - V_2''(y - x) + \frac{1}{D_2} [u_2 - V_2'(y - x)]^2 \right\} P_{1,1}^{1,N}(x, y) \\ & + \int_0^L dx dy dy' \frac{1}{D_1} \left(\frac{u_1}{N} - V_1'(x - y) \right) \\ & \times \left(\frac{u_1}{N} - V_1'(x - y') \right) P_{1,2}^{1,N}(x, y, y'), \quad (4) \end{aligned}$$

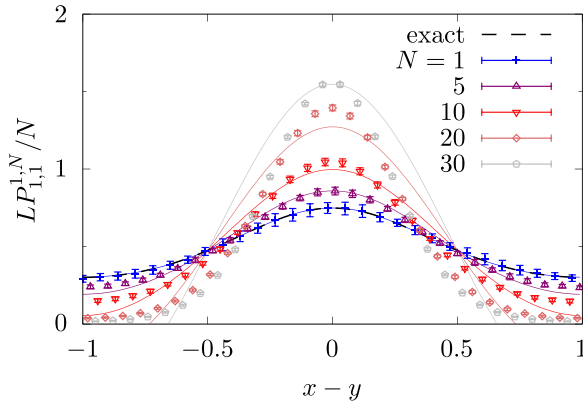


FIG. 2. Rescaled two-point correlation function $P_{1,1}^{1,N}(x, y)$ of A and B particles at x and y , with sinusoidal interaction potentials and $a_1 = -0.2$, $a_2 = -0.3$, $u_1 = u_2 = 0$, $D_1 = 1$, $D_2 = 0.1$, $L = 2$. Symbols show numerical estimates; dashed lines, exact result Eq. (5); and solid lines, perturbative prediction [37].

which is derived in the Supplemental Material (SM) [37], and where $P_{1,n}^{1,N}$ is the correlation function of an A particle and n B particles in a system of one A particle and N particles of type B. In the SM [37], we derive the entropy production in a more general system, namely, M particles of type A that interact with N particles of type B. We obtain Eq. (4) by setting $M = 1$. Equation (4) shows that the entropy production of this system depends on the two-point $P_{1,1}^{1,N}$ and three-point $P_{1,1,2}^{1,N}$ correlation functions [20]. In the absence of an exact solution, we calculate these correlation functions perturbatively, using a Doi-Peliti field theory that captures the Langevin dynamics in Eq. (1).

Two-particle system. The system with one particle of each species is tractable exactly. This is a model of a Janus dimer if V_1 and V_2 are chosen to be one attractive and the other repulsive, such that attractive forces dominate over repulsive forces [16–18]. Without self-propulsion, $u_1 = u_2 = 0$, the two-point correlation function is the barometric formula [36,38]

$$P_{1,1}^{1,1}(x, y) = \frac{1}{\mathcal{L}\mathcal{N}} e^{-\frac{V_1(x-y)+V_2(y-x)}{D_1+D_2}}, \quad (5)$$

with \mathcal{N} such that $\int_0^L dx dy P_{1,1}^{1,1}(x, y) = 1$, which is represented with dashed lines in Fig. 2. The three-point correlation function is naturally $P_{1,1,2}^{1,1} = 0$. Setting the currents to zero, $J_x = 0$ and $J_y = 0$, gives the condition for detailed balance for this system,

$$\frac{V_1'(x-y)}{D_1} = -\frac{V_2'(y-x)}{D_2}, \quad (6)$$

showing an equivalent role in the amplitude of interaction force and diffusion. *The system can therefore be out of equilibrium due to particle interactions even in the absence of self-propulsion.* The detailed balance condition in Eq. (6) is consistent with the detailed balance condition found in [1] for the special case of interactions modeled by harmonic oscillators and in [4] for interaction forces that differ by their amplitude. Using Eq. (5) in Eq. (4), the stationary entropy

production is

$$\dot{S} = \int_0^L d\ell \frac{\rho(\ell)}{D_1 + D_2} \left(\sqrt{\frac{D_2}{D_1}} V_1'(\ell) + \sqrt{\frac{D_1}{D_2}} V_2'(-\ell) \right)^2, \quad (7)$$

where $\rho(x-y) = LP_{1,1}^{1,1}(x, y)$. The entropy production is zero only if Eq. (6) is satisfied. In the case of a Janus dimer, Eq. (7) gives the average energetic cost of sustaining the structure and active motion of the colloid by laser light [16,17], according to Sekimoto's framework. Figure 3 shows \dot{S} for the two-particle case, $N = 1$, for sinusoidal interaction potentials.

Equilibrium system. Imposing the detailed balance condition in Eq. (6) and zero drifts $u_1 = u_2 = 0$, the stationary joint particle density is

$$P(x, y) = \frac{1}{\mathcal{L}\mathcal{N}} e^{-\sum_{i=1}^N \frac{V_1(x-y_i)+V_2(y_i-x)}{D_1+D_2}}, \quad (8)$$

with normalization \mathcal{N} such that $\int_0^L dx d^N y P(x, y) = N!$. The currents in Eq. (2) vanish, implying that the detailed balance condition in Eq. (6) generalizes to the many-particle system. This is an important result, though not surprising: by adding a new B particle to the equilibrium system, the system remains at equilibrium as long as the new particle satisfies the detailed balance condition stated above. Following the same procedure, we find that the detailed balance condition in Eq. (6) is general to the system with M particles of species A, as well as for the system with interactions between particles of the same species.

Chase and run. The limiting case where interaction forces between species are attractive-repulsive with equal magnitude and equal directions is of particular interest both for its biological motivation [13–15], as well as for its mathematical tractability. Assuming that interaction potentials satisfy $V_1(\ell) = -V_2(-\ell) \equiv V(\ell)$, the two-particle system is uniformly distributed, Eq. (5), because the distance $\ell = x - y$ diffuses in the comoving frame, and it is the center of mass that spins with velocity $-V'(\ell)$. By the same reasoning, the stationary joint particle density stays uniform when adding new B particles to the system. By marginalization, the $(1+n)$ -point correlation function is

$$P_{1,n}^{1,N}(x, y_1, \dots, y_n) = \frac{N!}{(N-n)!L^{n+1}}, \quad (9)$$

with $0 \leq n \leq N$. The entropy production in Eq. (4) is, thus,

$$\dot{S} = \frac{N}{L} \left(\frac{1}{D_1} + \frac{1}{D_2} \right) \int_0^L d\ell [V'(\ell)]^2, \quad (10)$$

yielding an exact result for arbitrary particle number N , shown in Fig. 3. Equation (11) shows that the system with chase-and-run dynamics is out of equilibrium independently of the magnitude of interaction forces. Indeed, the *chaser* tends to run behind the *chased*, exhibiting the breakdown of time-reversal symmetry.

Sinusoidal interaction potentials. To explore the parameter space of attractive and repulsive interactions, we consider sinusoidal potentials $V_1(\ell) = a_1 \cos k_1 \ell$ and $V_2(\ell) = a_2 \cos k_2 \ell$, with $k_1 = 2\pi/L$. The signs of a_1 and a_2 determine whether interactions are attractive or repulsive: negative amplitudes

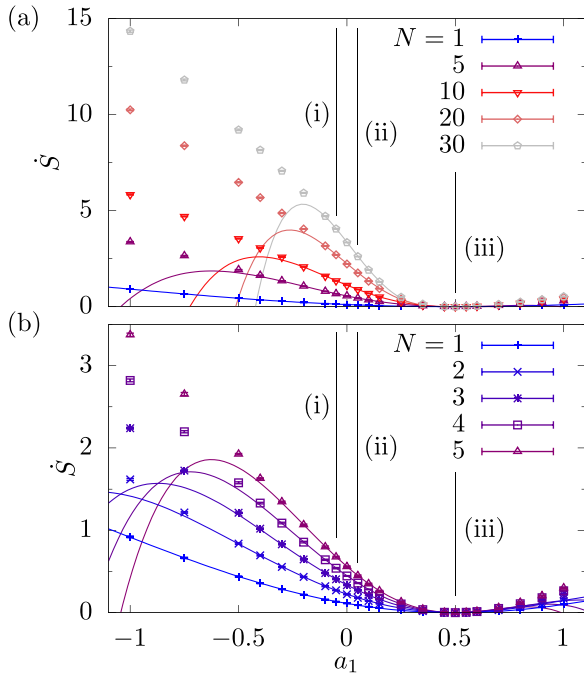


FIG. 3. Entropy production \dot{S} varying a_1 , (a) $N \in \{1, \dots, 30\}$ and (b) $N \in \{1, \dots, 5\}$, and fixed $a_2 = 0.05$, $D_1 = 1$, $D_2 = 0.1$, $u_1 = u_2 = 0$, $L = 2$. Symbols indicate numerical estimates using Sekimoto's framework, Eq. (11), and lines perturbative prediction in [37]. The cases (i) chase-and-run dynamics $a_1 = -a_2$, Eq. (10), (ii) reciprocal interactions $a_1 = a_2$, and (iii) equilibrium $a_1 = a_2 D_1/D_2$, are indicated. The system with reciprocal interactions is out of equilibrium because $D_1 \neq D_2$, Eq. (6).

result in attraction, whereas positive amplitudes result in repulsion, as shown in Fig. 1.

We derive the two-point and three-point correlation functions, in a perturbative expansion valid at small amplitudes a_1 and a_2 compared to the diffusion constants D_1 and D_2 in the SM [37]. In Fig. 2, we show the two-point correlation function $P_{1,1}^{1,N}(x, y)$ of the A particle at position x and one out of N particles of species B at y , as a function of the distance $x - y$, varying N , for fixed negative amplitudes $a_1 < 0$, $a_2 < 0$. Due to attractive interactions, short distances are favored over longer distances, which is more prominent as N increases. Figure 2 shows good agreement for small to intermediate N and illustrates how the deviation of the numerical estimates from the perturbative prediction increases with N .

Using the correlation functions $P_{1,1}^{1,N}$ and $P_{1,2}^{1,N}$ in Eq. (4) we obtain the entropy production \dot{S} , derived in the SM [37], which is shown in Fig. 3 as a function of a_1 (solid lines). The behavior of \dot{S} is shown for two ranges of N : the small to large particle number in Fig. 3(a), and the small to intermediate particle numbers in Fig. 3(b). Following Sekimoto's framework [1,25,34,35], in Fig. 3 we compare the perturbative result for \dot{S} with the total entropy production

$$\dot{S} = \frac{\dot{Q}_x}{\mathcal{T}_1} + \sum_{i=1}^N \frac{\dot{Q}_{y_i}}{\mathcal{T}_2} \quad (11)$$

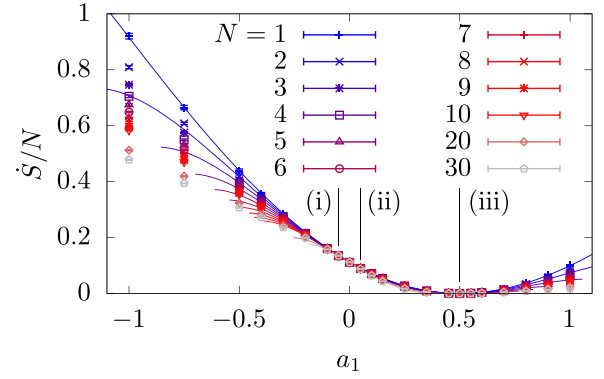


FIG. 4. Rescaled entropy production \dot{S}/N varying N and a_1 , for fixed $a_2 = 0.05$, $D_1 = 1$, $D_2 = 0.1$, $u_1 = u_2 = 0$, $L = 2$. The values of \dot{S}/N collapse onto a single point in case (i) chase-and-run dynamics ($a_1 = -a_2$) due to the linear dependence of \dot{S} in N , Eq. (10), and in case (iii) equilibrium ($a_1 = a_2 D_1/D_2$), where $\dot{S} = 0$. For any other values of a_1 , we find that \dot{S} grows sublinearly in N .

estimated numerically from the average rate of dissipated energy along particle trajectories, $\dot{Q}_x = \langle [\dot{x}(t) - \xi(t)] \circ dx(t) \rangle / dt$ and $\dot{Q}_{y_i} = \langle [\dot{y}_i(t) - \xi_i(t)] \circ dy_i(t) \rangle / dt$, where \circ denotes the Stratonovich product and where the temperatures are $\mathcal{T}_1 = D_1/(k_B \mu)$ and $\mathcal{T}_2 = D_2/(k_B \mu)$, with Boltzmann constant k_B and mobility μ set to unity.

The cases of chase-and-run dynamics, reciprocal interactions, and equilibrium are indicated in Fig. 3. Here, since the diffusion constants are different, $D_1 \neq D_2$, the system with reciprocal interactions does not satisfy the condition for detailed balance in Eq. (6) and is thus out of equilibrium. The agreement is excellent between numerical results and perturbative predictions within the validity regime, that is, for $|a_1|$ and N sufficiently small. Increasing either of those parameters leads to larger deviation of the numerical estimates from the perturbative prediction.

The entropy production \dot{S} shown in Fig. 3 corresponds to the system in the attractive-repulsive regime for $a_1 < 0$, and the repulsive-repulsive regime for $a_1 > 0$. We find that \dot{S} increases smoothly for amplitudes away from the equilibrium $a_1 = a_2 D_1/D_2$, as well as for increasing N . We also find that \dot{S} grows faster in the attractive-repulsive regime than in the repulsive-repulsive regime, showing that sustaining interaction forces with opposite sign (attractive-repulsive) is energetically more costly than forces with equal sign (repulsive-repulsive). This is reflected, for instance, in \dot{S} increasing as a_1 becomes more negative. Increasing the number N of B particles in the nonequilibrium system is an increase of the number of degrees of freedom, which leads to a larger entropy production rate, as shown in Figs. 3 and 4. In Fig. 4, the entropy production rate is rescaled by N . As predicted in Eq. (10), all curves coincide for $a_1 = -a_2$, showing a linear dependence of \dot{S} in N . We find that \dot{S} grows sublinearly in N for any $a_1 \neq -a_2$ and $a_1 \neq a_2 D_1/D_2$. This indicates that chase-and-run dynamics produce the highest average entropy \dot{S}/N in the limit of large N . Moreover, \dot{S}/N is bounded from above by the average entropy in the two-particle case ($N = 1$) for any a_1 , Eq. (7).

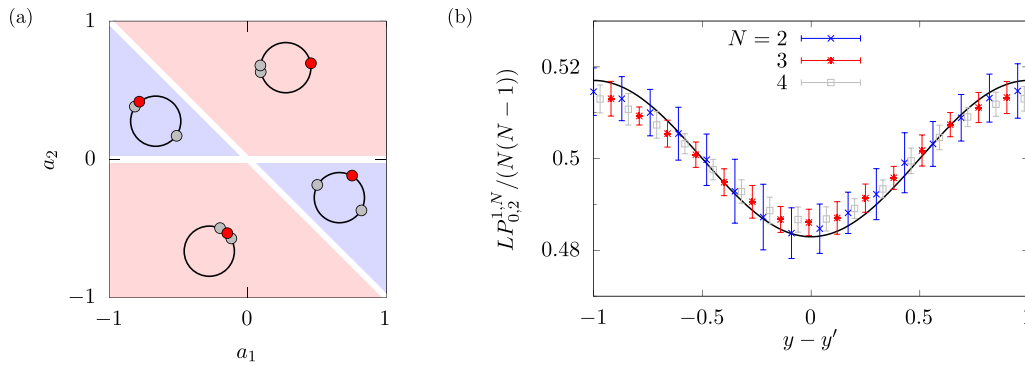


FIG. 5. Effective interactions between particles of species B. (a) Phase diagram showing effective attraction (red) and repulsion (blue) varying a_1 and a_2 , as predicted by the amplitude of the two-point correlation function $P_{0,2}^{1,N}(y, y')$ of two B particles at y and y' , in the presence of an A particle; insets show frequent configurations in each regime. (b) Rescaled $P_{0,2}^{1,N}$, with sinusoidal interaction potentials, and $a_1 = -0.2$, $a_2 = 0.15$, $D_1 = 1$, $D_2 = 0.1$, $u_1 = u_2 = 0$, $L = 2$. Symbols indicate numerical estimates, and solid line, perturbative result [37].

Effective interactions. Although particles of species B do not directly interact with each other according to Eq. (1), their trajectories are correlated through the particle of species A, as illustrated in Fig. 1. In Figs. 1(c) and 1(d), for instance, B particles visibly display effective attraction. Marginalizing the three-point correlation function, $\int_0^L dx P_{1,2}^{1,N}(x, y, y') = P_{0,2}^{1,N}(y, y')$, reveals correlations between any two particles of species B at positions y and y' , that we identify as effective interactions, with a sign (attractive or repulsive) that depends on the amplitudes a_1 and a_2 , derived in the SM [37]. We found that B particles display effective repulsion if $a_1 > -a_2 > 0$ or $-a_1 > a_2 > 0$ [blue area in the phase diagram in Fig. 5(a)], no correlation if $a_1 = -a_2$ or $a_2 = 0$ (white lines), and effective attraction otherwise (red area). Based on this prediction, which is of second order in the perturbation expansion, we explored the two-point correlation function $P_{0,2}^{1,N}$ for an example of effective repulsion in the regime $-a_1 > a_2 > 0$ [see Fig. 5(b)], which shows that long distances are more frequent than short distances between any two B particles. The underlying microscopic mechanism is the following: the attraction felt by particle A is stronger than the repulsion felt by B particles, so that A captures one of the B particles, while the rest escape.

Conclusions. We have studied the role of nonreciprocal interactions in the environmental entropy change using a fully microscopic theory. Our analytic results are an exact calculation of the entropy production rate of an interacting active many-particle system. Given the intrinsic relation between

entropy production and heat dissipation, our analytic prediction can be used to estimate the input energy required to sustain a specific pair of interparticle interaction forces that form and propel active colloids. Our model can be extended to include details of the self-propulsion and interaction mechanisms of a Janus dimer or an active colloidal molecule in a momentum-conserving solvent, by increasing the number of degrees of freedom. In that case, we expect the entropy production calculated from the richer description to be bounded from below by the entropy production calculated in this Letter. Our framework can be extended to estimate the extractable work in other physical systems, such as asymmetrically shaped objects immersed in active baths that have been proposed in the context of autonomous engines. While the asymmetric shape of the object can be captured in a suitable reciprocal interaction pair potential, the active motility of B particles can be implemented as an extension of the field theory derived in this Letter.

Acknowledgments. We are grateful to G. Pruessner for introducing us to field theory and for seminal discussions about the barometric formula. We also thank S. Loos, C. Scalliet, M. Cates, T. Agranov, P. Pietzonka, G. Biroli, B. Walter, L. Cocconi, and Z. Zhen for useful discussions. R.G.-M. was supported in part by the European Research Council under the EU's Horizon 2020 Programme (Grant No. 740269), and acknowledges support from a St John's College Research Fellowship, University of Cambridge.

- [1] S. Loos and S. Klapp, Irreversibility, heat and information flows induced by non-reciprocal interactions, *New J. Phys.* **22**, 123051 (2020).
- [2] C. Godrèche and J.-M. Luck, Characterising the nonequilibrium stationary states of Ornstein–Uhlenbeck processes, *J. Phys. A: Math. Theor.* **52**, 035002 (2019).
- [3] T. Kano, K. Osuka, T. Kawakatsu, and A. Ishiguro, Mathematical analysis for non-reciprocal-interaction-based model of collective behavior, *J. Phys. Soc. Jpn.* **86**, 124004 (2017).
- [4] A. V. Ivlev, J. Bartnick, M. Heinen, C.-R. Du, V. Nosenko, and H. Löwen, Statistical Mechanics where Newton's Third Law is Broken, *Phys. Rev. X* **5**, 011035 (2015).
- [5] A. Cavagna, I. Giardina, and T. S. Grigera, The physics of flocking: Correlation as a compass from experiments to theory, *Phys. Rep.* **728**, 1 (2018).
- [6] M. Nagy, Z. Ákos, D. Biro, and T. Vicsek, Hierarchical group dynamics in pigeon flocks, *Nature (London)* **464**, 890 (2010).
- [7] A. Deblais, A. Maggs, D. Bonn, and S. Woutersen, Phase Separation by Entanglement of Active Polymerlike Worms, *Phys. Rev. Lett.* **124**, 208006 (2020).
- [8] Z. You, A. Baskaran, and M. C. Marchetti, Nonreciprocity as a generic route to traveling states, *Proc. Natl. Acad. Sci. USA* **117**, 19767 (2020).

- [9] M. Fruchart, R. Hanai, P. B. Littlewood, and V. Vitelli, Non-reciprocal phase transitions, *Nature (London)* **592**, 363 (2021).
- [10] M. Durve, A. Saha, and A. Sayeed, Active particle condensation by non-reciprocal and time-delayed interactions, *Eur. Phys. J. E* **41**, 49 (2018).
- [11] L. Barberis and F. Peruani, Large-Scale Patterns in a Minimal Cognitive Flocking Model: Incidental Leaders, Nematic Patterns, and Aggregates, *Phys. Rev. Lett.* **117**, 248001 (2016).
- [12] S. A. M. Loos, S. H. L. Klapp, and T. Martynec, Long-Range Order and Directional Defect Propagation in the Nonreciprocal XY Model with Vision Cone Interactions, *Phys. Rev. Lett.* **130**, 198301 (2023).
- [13] S. Redner and P. L. Krapivsky, Capture of the lamb: Diffusing predators seeking a diffusing prey, *Am. J. Phys.* **67**, 1277 (1999).
- [14] C. Meredith, P. Moerman, J. Groenewold, Y.-J. Chiu, W. Kegel, A. van Blaaderen, and L. Zarzar, Predator-prey interactions between droplets driven by non-reciprocal oil exchange, *Nat. Chem.* **12**, 1136 (2020).
- [15] B. Stramer and R. Mayor, Mechanisms and *in vivo* functions of contact inhibition of locomotion, *Nat. Rev. Mol. Cell Biol.* **18**, 43 (2017).
- [16] F. Schmidt, B. Liebchen, H. Löwen, and G. Volpe, Light-controlled assembly of active colloidal molecules, *J. Chem. Phys.* **150**, 094905 (2019).
- [17] J. Grauer, F. Schmidt, J. Pineda, B. Midtvedt, H. Löwen, G. Volpe, and B. Liebchen, Active droplets, *Nat. Commun.* **12**, 6005 (2021).
- [18] R. Niu, A. Fischer, T. Palberg, and T. Speck, Dynamics of binary active clusters driven by ion-exchange particles, *ACS Nano* **12**, 10932 (2018).
- [19] E. A. Lisin, O. F. Petrov, E. A. Sametov, O. S. Vaulina, K. B. Statsenko, M. M. Vasiliev, J. Carmona-Reyes, and T. W. Hyde, Experimental study of the nonreciprocal effective interactions between microparticles in an anisotropic plasma, *Sci. Rep.* **10**, 13653 (2020).
- [20] G. Pruessner and R. Garcia-Millan, Field theories of active particle systems and their entropy production, [arXiv:2211.11906](https://arxiv.org/abs/2211.11906).
- [21] P. Gaspard, Time-reversed dynamical entropy and irreversibility in Markovian random processes, *J. Stat. Phys.* **117**, 599 (2004).
- [22] L. Cocconi, R. Garcia-Millan, Z. Zhen, B. Buturca, and G. Pruessner, Entropy production in exactly solvable systems, *Entropy* **22**, 1252 (2020).
- [23] H. Alston, L. Cocconi, and T. Bertrand, Non-equilibrium thermodynamics of diffusion in fluctuating potentials, *J. Phys. A: Math. Theor.* **55**, 274004 (2022).
- [24] U. Seifert, Stochastic thermodynamics, fluctuation theorems and molecular machines, *Rep. Prog. Phys.* **75**, 126001 (2012).
- [25] K. Sekimoto, *Stochastic Energetics* (Springer, New York, 2010), Vol. 799.
- [26] M. Brandenbourger, X. Locsin, E. Lerner, and C. Coulais, Non-reciprocal robotic metamaterials, *Nat. Commun.* **10**, 4608 (2019).
- [27] H. Alston, A. O. Parry, R. Voituriez, and T. Bertrand, Intermittent attractive interactions lead to microphase separation in nonmotile active matter, *Phys. Rev. E* **106**, 034603 (2022).
- [28] O. Granek, Y. Kafri, and J. Tailleur, Anomalous Transport of Tracers in Active Baths, *Phys. Rev. Lett.* **129**, 038001 (2022).
- [29] C. Maes, Fluctuating Motion in an Active Environment, *Phys. Rev. Lett.* **125**, 208001 (2020).
- [30] P. Pietzonka, É. Fodor, C. Lohrmann, M. E. Cates, and U. Seifert, Autonomous Engines Driven by Active Matter: Energetics and Design Principles, *Phys. Rev. X* **9**, 041032 (2019).
- [31] Z. Zhang and G. Pruessner, Field theory of free run and tumble particles in d dimensions, *J. Phys. A* **55**, 045204 (2022).
- [32] R. Garcia-Millan and G. Pruessner, Run-and-tumble motion in a harmonic potential: Field theory and entropy production, *J. Stat. Mech.* (2021) 063203.
- [33] M. Bothe, L. Cocconi, Z. Zhen, and G. Pruessner, Particle entity in the Doi-Peliti and response field formalisms, *J. Phys. A: Math.* **56**, 175002 (2023).
- [34] A. Ghosal and G. Bisker, Inferring entropy production rate from partially observed Langevin dynamics under coarse-graining, *Phys. Chem. Chem. Phys.* **24**, 24021 (2022).
- [35] É. Roldán, J. Barral, P. Martin, J. Parrondo, and F. Jülicher, Quantifying entropy production in active fluctuations of the hair-cell bundle from time irreversibility and uncertainty relations, *New J. Phys.* **23**, 083013 (2021).
- [36] H. Risken, *The Fokker-Planck Equation: Methods of Solutions and Applications*, 2nd ed. (Springer Verlag, Berlin, Heidelberg, 1989).
- [37] See Supplemental Material at <http://link.aps.org/supplemental/10.1103/PhysRevResearch.5.L022033> for details.
- [38] Z. Zhang, L. Fehértó-Nagy, M. Polackova, and G. Pruessner, Field theory of active Brownian particles in potentials, [arXiv:2212.12291](https://arxiv.org/abs/2212.12291).